Video Article

Sampling Strategies and Processing of Biobank Tissue Samples from Porcine Biomedical Models

Andreas Blutke[1], Rüdiger Wanke[1]

[1]Institute of Veterinary Pathology at the Centre for Clinical Veterinary Medicine, LMU Munich

Correspondence to: Andreas Blutke at blutke@patho.vetmed.uni-muenchen.de

URL: https://www.jove.com/video/57276
DOI: doi:10.3791/57276

Keywords: Medicine, Issue 133, Systematic Random Sampling, Quantitative Stereology, Orientator, Isotropic Uniform Random Section, Isector, Biobank, Porcine Model, Sample Processing, Volumetry, Embedding-Related Tissue Shrinkage

Date Published: 3/6/2018

Citation: Blutke, A., Wanke, R. Sampling Strategies and Processing of Biobank Tissue Samples from Porcine Biomedical Models. *J. Vis. Exp.* (133), e57276, doi:10.3791/57276 (2018).

Abstract

In translational medical research, porcine models have steadily become more popular. Considering the high value of individual animals, particularly of genetically modified pig models, and the often-limited number of available animals of these models, establishment of (biobank) collections of adequately processed tissue samples suited for a broad spectrum of subsequent analyses methods, including analyses not specified at the time point of sampling, represent meaningful approaches to take full advantage of the translational value of the model. With respect to the peculiarities of porcine anatomy, comprehensive guidelines have recently been established for standardized generation of representative, high-quality samples from different porcine organs and tissues. These guidelines are essential prerequisites for the reproducibility of results and their comparability between different studies and investigators. The recording of basic data, such as organ weights and volumes, the determination of the sampling locations and of the numbers of tissue samples to be generated, as well as their orientation, size, processing and trimming directions, are relevant factors determining the generalizability and usability of the specimen for molecular, qualitative, and quantitative morphological analyses. Here, an illustrative, practical, step-by-step demonstration of the most important techniques for generation of representative, multi-purpose biobank specimen from porcine tissues is presented. The methods described here include determination of organ/tissue volumes and densities, the application of a volume-weighted systematic random sampling procedure for parenchymal organs by point-counting, determination of the extent of tissue shrinkage related to histological embedding of samples, and generation of randomly oriented samples for quantitative stereological analyses, such as isotropic uniform random (IUR) sections generated by the "Orientator" and "Isector" methods, and vertical uniform random (VUR) sections.

Video Link

The video component of this article can be found at https://www.jove.com/video/57276/

Introduction

In translational medicine, pigs are increasingly common for use as large animal models[1,2,3,4,5], due to several advantageous similarities between the porcine and human anatomy and physiology, and the availability of established molecular biological methods allowing for generation of tailored, genetically modified pig models for a wide range of disease conditions[1,4].

However, compared to rodent models, the number of animals of a respective pig model that can be provided for experiments at any time is limited. This is due to the porcine generation interval of approximately one year, and the financial and time-intensive efforts required for the generation of porcine models and animal husbandry. Therefore, individual animals of a porcine model, as well as the samples that can be generated from these pigs, are very valuable, particularly if genetically modified porcine models and/or long-term experimental issues (*e.g.*, late complications of chronic diseases) are examined in aged individuals[2,6,7].

In the course of any study, performance of additional analyses which had not been scheduled in the initial experimental design of the study might later turn out to be relevant, *e.g.*, to address distinct questions arising from previously discovered unexpected findings. If suitable samples for such additional experiments are not available, disproportionally high cost and time-intensive expenditures might be necessary to generate additional pigs and tissue samples. To be prepared for such eventualities, generation of biobank collections of conserved back-up samples of different organs, tissues, or bio-liquids, quantitatively and qualitatively suitable for a broad range of subsequent analyses, is considered an important approach[2,6,7]. Deriving optimal benefits from a porcine animal model, the availability of adequate biobank samples also offers the unique possibility to perform a broad spectrum of different analysis methods on identical sample materials on a multi-organ level in the very same individual animals, *e.g.*, by distribution of samples to scientists of different working-groups organized in a research network[2,6,7]. Additionally, the "forward-looking" sampling strategy in biobanking also contributes to a reduction of the number of animals needed in a study. The advantages of porcine model biobanking have recently been demonstrated in a multi-organ, multiomics study, examining organ cross talk in a genetically modified porcine model of long-term diabetes mellitus, using specimens from the Munich MIDY Pig Biobank[2].

There are some mandatory requirements biobank samples must generally comply with to establish the reliability and interpretability of the results of the subsequently performed analyses. The samples must be generated reproducibly, and they must be representative, *i.e.*, adequately reflecting the interested morphological and molecular features of the tissue/organ the samples were taken from[7]. To be suitable for a wide range of downstream analysis types, the samples must be taken in sufficient quantities and processed according to the demands (including time and temperature conditions) of the different analytical methods, including descriptive histopathological analyses, such as cryohistology, paraffin and plastic histology, immunohistochemistry, *in situ* hybridization, ultrastructural electron microscopic analyses, and clinical laboratory diagnostic analyses, as well as molecular analyses of DNA, RNA, proteins, and metabolites.

To allow for the assessment of a wide range of distinct quantitative morphological parameters such as numbers, volumes, lengths, or surface areas of distinct tissue structures by quantitative stereological analyses, randomized section planes of the histological samples of the respective organs/tissues need to be prepared[7,8,9,10,11]. In quantitative morphological studies, the precise determination of the total volume of the tissue, organ, or organ compartment, the samples were taken from (*i.e.*, the reference space) is crucially important[7,9,12] to calculate the absolute quantities of the interested parameters within the respective organ, tissue, or organism. Eventually, the effect of embedding-related tissue shrinkage during preparation of histological sections has to be determined and taken into account[13]. Therefore, quantitative stereological analyses, especially of archived samples (fixed tissue samples, embedded tissue blocks, histological sections, *etc.*) from previous studies are sometimes severely limited or even impossible[12], particularly if volumetry of the respective organs/tissues was not performed, if no adequate sampling designs were applied to warrant representative samples, if the numbers and amounts of available individual samples are insufficient, or if the processing of the samples is incompatible with estimation of the quantitative morphological parameter(s) of interest. Due to the manifold possible influencing factors, the suitability of archive-sample materials for analyses of distinct quantitative morphological parameters cannot unequivocally be answered, but depends on the careful assessment of each individual case.

Thus, as the location, size, number, processing, trimming direction, and orientation of samples will potentially affect the results of the subsequent analyses, these factors are of great importance and must be considered in the experimental design of any study. With regard to these aspects and the special features of the porcine anatomy, comprehensive, detailed, large-scale sampling guidelines adapted to porcine animal models have recently been established, providing a robust reference to standardized, reproducible, and efficient generation of redundant, adequately processed, high-quality samples from more than 50 different porcine organs and tissues[6,7].

The methodological descriptions and the video tutorial shown in the present article provide detailed, illustrative, comprehensible, step-by step instructions for practical performance of a variety of techniques for volumetry, sampling of porcine tissues and organs, and processing of tissue samples for different downstream analysis methods. The featured techniques include methods for determination of organ/tissue volumes and densities based on the principles of Archimedes and Cavalieri[9], including determination of the dimensions of three-dimensional shrinkage of tissue related to the embedding in different embedding media[14] during processing for histological examination, application of practicable volume-weighted systematic random sampling approaches, processing of sampled tissue specimens for different subsequent analyses[7,8,9,15], and generation of appropriately oriented and processed samples for potential quantitative stereological analyses[7,8,9,10,11]. Next to their application in porcine biobank projects, the demonstrated methods are generally appropriate for all studies examining quantitative histo-morphological properties of organs/tissues. Moreover, systematic random sampling designs are particularly beneficial for generation of representative samples in experiments using molecular analysis methods to detect abundance alterations of, *e.g.*, RNAs, proteins, or metabolites in various organs and tissues.

The next paragraphs provide a brief introduction to these methods, while their practical performance is described in the protocol section.

Determination of organ/tissue volumes
Determination of organ weights and volumes is important in several experimental settings, as these factors might indicate changes, potentially related to experimentally examined factors of interest. The total volume of an organ/tissue is also commonly required to calculate absolute quantitative parameters, (*e.g.*, the total cell number), from stereologically estimated numerical volume densities (*i.e.*, the number of cells per volume unit of tissue)[7,12]. Apart from techniques using complex technical equipment, such as computer tomography, there are basically three practical methods commonly used to determine the absolute volume of an organ or tissue. The volume of an organ can be determined by "direct volumetric measurement" according to the principle of Archimedes, *i.e.*, measuring the volume of water or saline displaced by the structure when completely submerged. However, for comparably large porcine organs, these approaches are impractical and prone to imprecision, since they require very large volumetric/measuring flasks. More conveniently, the volume of an organ/tissue can be calculated from its weight and density[7,12,16], which can efficiently be determined using the "submersion method"[7,12,16] (protocol step 1.1.). Organ/tissue volumes can also be estimated using volumetry approaches based on the "principle of Cavalieri" (1598–1647). In simple terms, the Cavalieri principle states, that if two objects are sectioned in planes parallel to a ground plane, and the profiles of the sections cut through the two objects at corresponding distances from the ground plane have the same areas, the two objects have the same volume. Thus, the volume of arbitrarily shaped objects can be estimated as the product of their section profile areas in parallel, equally distant section planes and the distance between the section planes. This is comprehensible with the following analogy: consider two stacks consisting of the same number of identical coins are placed side by side, one stack with the coins orderly stacked on top of one another yielding a cylindrical shape of the coin stack, and the other stack of coins with off-center positioned coins (**Figure 3A**). Although the shapes of both coin stacks are different, their volumes are the same, since the areas of the coins at corresponding levels of both stacks (*i.e.*, the areas of profiles of parallel sections cut through both coin stacks in equal distances from the ground) are identical. Estimation of the volumes of porcine organs and tissues using the Cavalieri principle[7,12,15] is described in step 1.2.

Determination of the extent of tissue shrinkage related to histological embedding
In analyses of several quantitative morphological parameters measured in histological tissue sections, the effect of embedding-related tissue shrinkage occurring during tissue processing for histology has to be determined and taken into account. The extent of embedding-related tissue shrinkage may be variable, and depends both on the tissue, its processing, and the embedding medium[8,13,17,18,19]. Generally, embedding-related changes of the volume of a tissue sample (*i.e.*, mostly shrinkage) occur in all three dimensions of space, and, therefore, affects all dimensional parameters estimated by quantitative stereological analyses[8]. Basically, the extent of embedding-related tissue shrinkage, expressed as the linear tissue shrinkage factor (f_S), can be estimated as shown in step 1.3. and used for correction of (shrinkage-sensitive) quantitative morphological parameters[14].

Volume-weighted systematic random sampling of organs/tissues

For establishment of a biobank collection of porcine organ/tissue samples, volume-weighted systematic random sampling approaches such as described in step 2 have proven to be practical, time-saving, and efficient techniques for generation of representative, multi-purpose tissue samples[7,8,9,15].

Generation of Isotropic Uniform Random sections and Vertical Uniform Random sections for quantitative stereological analyses
Biobank tissue samples need to be suitable for a wide range of different quantitative stereological analysis methods for estimation of a maximum of parameters that could not be determined without an adequately prepared specimen. Nearly all quantitative stereological parameters can be determined, using "isotropic (independent) uniform random (IUR) sections"[8,9]. In IUR sections, the three-dimensional orientation of the section plane of the tissue sample is randomized. This can be achieved by randomization of the position of the tissue sample relative to the position of the section plane, as applied in the "Isector" method[11] (protocol step 3.1), or by randomization of the orientation of the section plane relative to the tissue sample, as in the "Orientator" method[10] (protocol step 3.2). In tissue samples, such as skin- or mucosa specimen displaying a naturally present, or defined and properly identifiable vertical axis, preparation of "vertical uniform random (VUR) sections" (protocol step 3.3.) strictly sectioned within the plane of their vertical axis is advantageous[8,20]. For a complete discourse of the theoretical foundations of IUR/VUR sampling and a comprehensive discussion of potential downstream quantitative stereological analyses, the interested reader is referred to the textbooks of quantitative stereology in life sciences[8,9].

Protocol

All methods described here use tissue samples derived from dead animals and fully comply with the German legal regulations of animal welfare.

1. Volumetry

1. **Submersion Technique for Determination of Tissue/Organ Densities (Figure 1 and Figure 2)**[7,12,16]
    1. Prepare materials: Scalpel blades, paper towels, fine forceps, standard laboratory scales, glass or plastic beakers, 0.9% saline, and self-constructed specimen holders (**Figure 2A**).
    2. Excise a piece of tissue (maximum size: 2 x 2 x 2 cm^3) from the organ/tissue, specifically from the organ compartment of interest. Small organs, such as the pituitary, or the pineal gland, are measured *in toto*.
    CAUTION: Ensure that the size of the sample is notably smaller than the inner diameter of the beaker (step 1.1.5 *et seq.*), and its filling level to allow complete submersion of the sample without contacting the inner walls of the beaker in step 1.1.7.
    3. Carefully swab the sample with a paper towel to remove excess blood/tissue fluid.
    4. Weigh the sample on a precision scale and record the weight of the sample (m_S). Determine the weight of small tissue samples to the nearest mg (**Figure 1A**).
    5. Place a beaker filled with room-temperature 0.9% saline on the scale. Do not completely fill the beaker, to allow for a submersion of the tissue sample in the subsequent step without overflowing.
    CAUTION: Use a beaker size appropriate to the size and weight of the tissue sample(s) to be measured and the effective measurement range of the scale. For larger samples up to 2 x 2 x 2 cm^3, a beaker size of 50–100 mL is appropriate in combination with a scale measuring from approximately 100 mg to 500 g, whereas for small samples, use beakers of 5–10 mL volume in combination with precision scales with measuring ranges between approximately 0.1 mg and 20 g.
    6. Submerge the sample holder (*i.e.*, a sufficiently rigid loop of thin wire or something similar, **Figure 2A**) in the saline to a marked position (arrows in **Figure 1B**, **Figure 2B**, and **Figure 2C**). Then, reset (tare) the display of the scale to zero.
    7. Carefully attach the tissue sample to the sample holder and completely submerge the sample in the saline until the marked position on the sample holder is reached (arrows in **Figure 1B**, **Figure 2B**, and **Figure 2C**).
    CAUTION: The submerged sample and the sample holder must not have contact with the inner walls or the bottom of the beaker or the surface of the saline.
    8. While holding the sample holder and the submerged sample in that position, record the weight displayed on the scale (m_L), referring to the weight of saline displaced by the tissue sample (**Figure 1C**, **Figure 2B**, and **Figure 2C**).
    9. Calculate the volume of the sample (V_S) from m_L, and the density of saline at room temperature (20 °C) (ρ_{saline} = 1.0048 g/cm^3) as $V_S = m_L/\rho_{saline}$ [g/g/cm^3] (**Figure 1**).
    10. Calculate the density of the tissue sample (ρ_{sample}) from the weight (*i.e.*, mass) of the sample (m_S) and its volume (V_S): $\rho_{sample} = m_S/V_S$ [g/cm^3] (**Figure 1**).
    11. For organs measured *in toto*, repeat the measurement three times and calculate the average organ density from the single measurement values. For large organs/tissues, perform repeated measurements with different samples of the same organ/tissue/organ compartment, and calculate the average density from the single measurements, accordingly.
    12. Calculate the total volume of the organ/tissue/organ compartment from its weight and density (**Figure 1**).

2. **Application of the Cavalieri-Method for Determination of Porcine Organ Volumes**[7]
    1. Prepare materials: Ruler, caliper, knife, scissors, forceps, waterproof pen, plastic transparencies, scanner, photo camera, and cross grids printed on plastic transparencies.
    2. Place the entire organ/tissue on a plain surface (cutting base) and measure the length (l) of the organ along its longitudinal axis (**Figure 3B**, **Figure 5A**).
    3. Cut the complete organ/tissue into equidistant parallel slices orthogonal to the longitudinal organ axis (**Figure 3C**, **Figure 5B**). Choose a distance d between two sections (*i.e.*, the sectioning interval/section thickness, usually approximately 1 cm) sufficiently small to receive a sufficient number of tissue/organ slabs. Randomly position the first section within a distance between 0 and the sectioning interval from the margin of the organ. While slicing, visually judge the position and orientation of each section plane, to obtain approximately parallel organ/tissue slabs of roughly uniform thickness.
    NOTE: The necessary number of tissue/organ slabs depends on the shape and the size of the examined organ/tissue. If small organs or samples have to be sectioned in thin slabs of ≤5 mm, embed the samples in agar prior to sectioning (see step 1.3.3.) and use a technical device for slicing of the agar-embedded sample. Empirically recommendable sectioning intervals for most porcine organs and

tissues, as well as examples for slicing devices, are indicated in the Supplementary Material of "Tissue Sampling Guides for Porcine Biomedical Models"[7].

4. Place all organ/tissue slabs on the same surface facing down on the cutting base (*i.e.*, consistently on either the right or the left section plane of each organ slab, **Figure 3D**, **Figure 5C**) and count the slabs (*n*).
5. Obtain section profiles of the tissue slabs by one of the following approaches:
    1. Carefully place the tissue slabs on appropriately labeled plastic transparencies, while maintaining the orientation of their upper and lower section surfaces. Trace the outlines of the tissue slabs on the plastic transparencies using a waterproof pen (**Figure 3E1-2**).
    2. Take photographic images of the tissue slabs, holding the camera vertically above the section surfaces (**Figure 3F**). For calibration, place a size ruler next to the tissue slabs.
    3. Scan the tissue slabs on a flatbed scanner while maintaining the orientation of their upper and lower section surfaces (**Figure 3G**). For calibration, place a size ruler next to the tissue slabs.
6. Measure the areas of the (traced, photographed, or scanned) section profiles of all tissue slabs by one of the following approaches:
    1. Overlay or superimpose the traced organ slab profiles with an appropriately sized, calibrated grid of equally spaced crosses printed on a plastic transparency and count all crosses hitting the profile area (**Figure 3E3-4**; compare to **Figure 5D**). Calculate the section profile area of each organ slab by multiplying the number of crosses hitting the profile area by the area corresponding to one cross.
    NOTE: To receive sufficiently precise volume estimates, choose a cross grid with a sufficiently small distance between adjacent crosses, so that an average of at least 100 crosses will hit the section surfaces of the slabs of one organ in each examined case of the study. Empirically recommendable cross grid sizes for most porcine organs and tissues are indicated in the Supplementary Material of "Tissue Sampling Guides for Porcine Biomedical Models"[7].
    2. Measure the areas of the tissue slabs in the digital images of the photos/scans using appropriate commercially available or freeware morphometry soft- and hardware applications (**Figure 3H**), such as a commercial image analysis system[21], or ImageJ[22].
    CAUTION: Note that one tissue slab (either the first or the last) is placed on the scanner resting on its natural surface, respectively, faces the camera with its natural surface. Therefore, the scanned image, the photo image of this slab, will not show a section surface. Therefore, no section area profile is measured in the scanned image/photo image of this tissue slab (**Figure 3I**). Also note over-projection present in scanned images and photographs of organ/tissue slabs, *i.e.*, only measure the areas of the actual section profiles, but not of the tissue in the image lying behind the slab section surface (**Figure 12G-H**).
7. Calculate the estimated organ volume as the product of the sum of all corresponding section profile areas of all tissue slabs per case (*i.e.*, consistently of either the right or the left, respectively, the upper or lower section surface of each organ slab and the mean thickness of the slabs (*i.e.*, the quotient of the measured length of the vertical organ axis (l) and the number of slabs)[15].

3. **Determination of the Extent of Three-Dimensional Embedding-Related Tissue Shrinkage during Processing of Tissue Samples for Histology**
    1. Prepare materials: Microtome blades, forceps, agar, metal casting molds, digital scanner, and size ruler (*e.g.*, graph paper).
    2. Cut a fresh, plane section surface from a fixed tissue sample.
    NOTE: If using samples of easily deformable (soft) tissues (fat tissue, gelatinous tissues), embed the fixed tissue sample in agar prior to sectioning (**Figure 4A**).
    3. To embed sample in agar:
        1. Mix standard agar powder as used for microbiology culture medium with an appropriate volume of water (approximately 0.5–1 g agar/10 mL water) in a glass beaker. Stir the mixture and heat it in a microwave oven at 700 W until boiling for 3–5 s. Stir the mixture and bring to a boil again for 3–5 s.
        2. Optionally, to increase the contrast of the agar to the tissue sample, dye the liquid agar, *e.g.*, with black ink (add 1 mL ink to 10 mL of hot liquid agar and stir vigorously).
        3. Pour the hot agar into a casting mold (*e.g.*, a metal mold used for paraffin embedding, **Figure 10A-D**) and submerge the fixed tissue sample in the warm agar. Let the agar cool until solidification, remove the mold, and cut the agar block with the embedded tissue using a microtome or razor blade.
        CAUTION: While handling hot liquid agar, wear protective goggles and gloves. Process tissue samples fixed in formaldehyde solution under an exhaust hood and wear protective goggles and laboratory gloves.
    4. Place the sample with its section surface facing down on a flatbed scanner, together with a size ruler and scan the section surface (**Figure 4A,B**).
    5. Determine the area of the section surface of the fixed tissue sample (A_f) in the digital scan, using one of the techniques described in step **1.2.6** (**Figure 4B**).
    6. Embed the sample in plastic embedding medium, such as epoxy (*e.g.*, Epon) or glycolmethacrylate/methylmethacrylate (GMA/MMA)[23], following standard protocols[23,24,25] (**Figure 4C**). Ensure that the section surface of the fixed sample scanned in the previous step (1.3.4) is maintained in the plastic-embedded sample.
    NOTE: To maintain the orientation of the section surface of the sample during processing of the sample, consistently place the sample with its intended section surface facing downwards into the embedding cassette or the casting mold, or mark the intended section surface (or the opposite side of the sample) with ink.
    7. Cut a histological section from the plastic block corresponding to the original section surface of the fixed tissue sample (step 1.3.2) using a microtome (**Figure 4D**), mount the section on a glass slide (**Figure 4D**) and stain it routinely (*e.g.*, Hematoxylin and eosin stain, H&E)[24,25].
    CAUTION: To receive a histological section approximately in the same plane as the original section surface of the fixed tissue sample, carefully adjust the position of the plastic block in the mount of the microtome before sectioning.
    8. Place the slide with the stained section facing downwards on a flatbed scanner together with a size ruler and scan the section (**Figure 4E**).

9. Determine the area of the section of the plastic-embedded tissue sample (A_e) in the digital scan, using one of the techniques described in step 1.2.6 (**Figure 4F**).
10. Calculate the average embedding-related tissue shrinkage (for the respective tissue and embedding medium) from the measured areas of corresponding section profiles of tissue samples before and after embedding in plastic embedding medium. The linear shrinkage factor f_s is calculated as the square root of the quotient of the areas of the section profiles of *n* tissue samples after embedding in plastic embedding medium (A_e) and the areas of the corresponding section profiles of the same tissue samples before embedding in plastic embedding medium (A_f) (**Figure 4G**)[14].

2. Volume-weighted Systematic Random Sampling by Point Counting and Processing of Tissue Subsamples for Different Downstream Analysis-types[7]

1. Prepare materials: Ruler, caliper, knife, scissors, forceps, waterproof pen, point/cross grids printed on plastic transparencies, and random number tables.
   NOTE: Copy templates for cross grids (5–60 mm) are provided in the Supplementary Material of "Tissue Sampling Guides for Porcine Biomedical Models"[7].
2. Place the organ/tissue on a plain surface (cutting base) and measure the length (*l*) of the organ along its longitudinal axis (**Figure 5A**, **Figure 6A**).
3. Cut the complete organ/tissue into equidistant parallel slices orthogonal to its longitudinal axis (**Figure 5B**). Choose a distance *d* between two sections (*i.e.*, the sectioning interval/section thickness, usually approximately 1 cm) small enough to obtain a sufficient number of tissue/organ slices. Randomly position the first section within a distance between 0 and the sectioning interval from the margin of the organ. While slicing, visually judge the position and orientation of each section plane to obtain approximately parallel organ/tissue slabs of roughly uniform thickness.
   NOTE: The necessary number of tissue/organ slabs depends on the size of the examined organ/tissue and the number of sampled tissue locations. If small organs or samples have to be sectioned in thin slabs of ≤5 mm, embed the samples in agar prior to sectioning (see step 1.3.3.) and use technical devices for slicing of the agar-embedded sample. Empirically recommendable sectioning intervals for most porcine organs and tissues, as well as examples for slicing devices are indicated in the Supplementary Material of "Tissue Sampling Guides for Porcine Biomedical Models"[7].
4. Place all organ/tissue slabs on the same surface facing down on the cutting base (**Figure 6B**).
5. Overlay the tissue slabs with an appropriately sized cross grid printed on a plastic transparency by placing the outermost left upper cross of the grid over a random point out of the tissue (**Figure 5C-D**, **Figure 6B**).
   NOTE: Choose a cross grid with a sufficiently small distance between adjacent crosses, so that in each examined case of the study, at least twice as many crosses will hit the section surface(s) of the tissue compartment to be sampled, as the number of samples that have to be taken from that tissue compartment. Empirically recommendable cross grid sizes for most porcine organs and tissues are indicated in the Supplementary Material of "Tissue Sampling Guides for Porcine Biomedical Models"[7].
6. Mark and count all crosses hitting the tissue (respectively, the tissue sub-compartment to be sampled). Consistently apply a uniform mode of counting and numbering of the crosses hitting the tissue compartment to be sampled in all tissue slabs, *e.g.*, by consecutive numbering of the respective crosses in each line by line, from the left to the right and from top to bottom, or, *e.g.*, by numbering the crosses in one tissue slab after another in clockwise direction, starting with the cross closest to the twelve o'clock position, as exemplarily demonstrated in **Figure 5E**.
7. Divide the number of crosses hitting the tissue/tissue compartment to be sampled (*n*) by the number of samples to be generated to obtain the systematic sampling interval (*i*).
8. Determine the first sampling position by choosing a random number *x* in the interval between 1 and *i*. For this, use a random-number table. Mark the first sampling position (*x*) and every next $x + i$, $x + 2i$, $x + 3i$, *etc.,* cross hitting the tissue/tissue compartment to be sampled on the plastic transparency using a waterproof pen (**Figure 5F**).
   NOTE: Random number tables can be conveniently and quickly generated using an online random number generator.
9. Tag the tissue locations corresponding to the marked crosses by slightly raising the plastic transparency and placing a small piece of clean, blank confetti paper on the surface of the tissue slab using a pair of tweezers (**Figure 5G**, **Figure 6E**).
10. Excise specimen of tissue from the sampled locations (**Figure 5H**, **Figure 6F**, **Figure 7A**) and further subdivide them for different types of subsequent analyses (**Figure 6G**, **Figure 7A**-B), as specified in **Table 1**.
11. After sampling, clean the plastic transparencies with warm water and soap, dry, and reuse them.

3. Generation of Isotropic Uniform Random (IUR) Sections and Vertical Uniform Random (VUR) Sections for Quantitative Stereological Analyses

1. **"Isector" Technique**
   1. Prepare materials: Razor or microtome blades, agar, spherical casting molds (*e.g.*, casting molds for pralines, which can be obtained from confectioner suppliers), foldback clamps, and forceps.
   2. Place an adequately sized piece (1 x 1 x 1 cm^3) of fixed, systematically randomly sampled tissue in a spherical casting mold, hold together by foldback clamps, and fill the mold with warm liquid agar (**Figure 8A-E**).
   3. Remove the agar sphere (**Figure 8F**) from the casting mold after solidification of the agar.
   4. Roll the agar sphere with the embedded tissue sample across the table, stop, and section it at a random position.
      NOTE: The resulting section plane is an IUR section (**Figure 8F-G**).
   5. Proceed to embed the tissue sample in plastic resin such as GMA/MMA, maintaining the orientation of the IUR section plane (see 1.3.5).

2. **"Orientator" Technique**
   1. Prepare the materials: Razor or microtome blades, agar, forceps, random number table(s), prints of equiangular, and cosine-weighted circles.

NOTE: Copy templates of circles are provided in previous publications[8,26].

2. Place the sample of fixed tissue (or of agar-embedded fixed tissue) on a print of an equiangular circle with one edge parallel to the 0–180° direction (**Figure 9A**, **Figure 10E**).
3. Determine a random angle by using the random number table. Find the corresponding marks at the scale of the equiangular circle, which the sample rests on. Using these marks, cut a section through the sample (or through the agar surrounding the embedded tissue sample), with the section plane being oriented parallel to the direction of the random angle indicated on the scale of the equiangular circle, and vertical to the resting surface of the sample (**Figure 9B-C**, **Figure 10F**).
4. Place the tissue block with the section surface generated in the previous step facing downside on a cosine-weighted circle with the edge of the resting surface placed parallel to the 1-1 direction (**Figure 9D**, **Figure 10H**).
5. Repeat step 3.2.3 and cut a new section through the sample at a random angle determined using the random number table (**Figure 9E-F**, **Figure 10I-J**).
   NOTE: The resulting section plane is an IUR section.
6. If appropriate, determine the area of the IUR section profile of the fixed tissue sample for determination of the embedding-related tissue shrinkage (**Figure 9G-J**) as described in step 1.3, and proceed to embed the tissue sample in plastic resin such as GMA/MMA.

3. **Generation of Vertical Uniform Random (VUR) Sections**
   1. Prepare materials: Razor or microtome blades, agar, forceps, random number table(s), and prints of equiangular circles.
      NOTE: Copy templates of circles are provided in previous publications[8,26].
   2. Define a vertical axis within the fixed tissue sample that is always recognizable in the sample/sections during the subsequent steps.
      NOTE: Typically, the axis vertical to the natural surface of the tissue sample is chosen as the vertical axis.
   3. If appropriate, embed the sample in agar (**Figure 11B**).
      NOTE: Agar-embedding prior to VUR- or IUR-sectioning of the fixed sample is generally recommendable for small, thin, fragile, or soft samples. Also use agar-embedding of samples to facilitate the positioning of the VUR sectioned sample during the subsequent embedding of the sample in plastic resin medium.
   4. Place the sample on a print of an equiangular circle, with the vertical axis being orthogonally oriented to the plane of the table/paper table (**Figure 11C**).
   5. Cut the sample at a random angle (determined using a random number table) with the section plane orthogonal to the table and parallel to the vertical axis to receive a VUR section plane (**Figure 11D**).
   6. If appropriate, determine the area of the IUR section profile of the fixed tissue sample for determination of the embedding-related tissue shrinkage as described in step 1.3 (compare to **Figure 9G-J**) and proceed to embed the tissue sample in plastic resin such as GMA/MMA.

Representative Results

Submersion technique for determination of tissue/organ density

Figure 12A-B shows the representative determination of the density and volume of a porcine kidney using the submersion technique described in step 1.1 (**Figure 1**, **Figure 2**). More representative results of density measurements of additional porcine organs and tissues are presented in **Table 2**. A more comprehensive list of reference densities of diverse porcine tissues and organs is shown in the "Tissue Sampling Guides for Porcine Biomedical Models"[7]. The validity of tissue density measurement values obtained using the submersion method may be estimated by repeated measurements of the same sample and of independent specimens. Most porcine tissues display density values slightly higher than water ($\rho_{water} \approx 1.0$), whereas tissues swimming in saline (adipose tissue, lung tissue) display densities <1.0.

Cavalieri method for determination of organ volumes

Figure 12C-F shows the representative determination of the volume of porcine kidney (the same organ as shown in **Figure 12A-B**). The areas of the section surfaces of the organ slabs were determined by point-counting, using a superimposed cross grid printed on a plastic transparency, as well as by planimetric measurement of the section areas of organ slabs in a scanned image of the slabs (paying attention to over-projection of tissue located behind the slabs section surfaces, **Figure 12 G-H**). The accuracy of organ/tissue volume data obtained by performance of the Cavalieri approach (step 1.2, **Figure 3**) may be estimated by comparison to the respective volume calculated from the weight and density of the organ/tissue. The volumes of the kidney examined in **Figure 12** determined by the submersion-method and the Cavalieri method(s) differed by less than 1% from each other. As a measure of the accuracy of the Cavalieri volume estimates, its coefficient of error (CE) can be calculated, as described earlier[15].

Determination of Three-dimensional Embedding-related Tissue Shrinkage during Processing of Tissue Samples for Histology

Representative results of the extent of tissue shrinkage related to embedding of porcine tissue samples (cortical renal tissue) in plastic resins (GMA/MMA or epoxy) for quantitative histomorphological examination are shown in **Table 2** (previously unpublished data). The linear shrinkage factors indicated in **Table 2** were determined as described in step 1.3 (**Figure 4**). They refer to a three-dimensional volume reduction of 29% for GMA/MMA embedding, and 22% for epoxy embedding of porcine cortical renal tissue. **Figure 13** shows representative examples of adequately and insufficiently prepared samples of agar-embedded, formalin-fixed adipose tissue for measurement of the sample section surface area prior to plastic-embedding.

Volume-weighted Systematic Random Sampling by Point Counting and Processing of tissue Subsamples for Different Downstream Analysis Types

The "sectioning and point-counting" technique for volume-weighted systematic random sampling of parenchymal organs (step 2, **Figure 5**, **Figure 6**, **Figure 7**) represents an established, robust method for generation of representative samples for multiple subsequent types of analyses[2,7]. Representative results of generation of systematically randomly sampled, highly redundant biobank specimen of various porcine organs and tissues, with subsequent differential processing of the excised tissue samples for multiple different downstream analysis methods using the sampling technique described in step 2 (**Figure 5**, **Figure 7**, and exemplarily demonstrated in **Figure 6**) have previously been published[2]. For generation of biobank samples of liver tissue in a previous porcine biobank study[2], for example, porcine livers were completely sectioned into approximately 20 slabs of 2 - 3 cm thickness, superimposed with a with a 3 cm cross grid, as described in step 2, and 16 tissue locations of approximately 2 x 2 x 2 cm^3 were systematically randomly sampled and excised in each case. From each of the excised samples, five subsamples were subsequently generated for molecular analyses (frozen at -80 °C) of sampled locations, one subsample for cryohistology, one subsample was fixed in Methacarn solution, and one in formaldehyde solution for subsequent paraffin embedding and histological- and immunohistochemical examination. The generation of the 74 different samples per case (until freezing or transfer of the samples into fixation solution) was achieved within approximately 20 min, on average[2]. The practicability/success of the described sampling and subsampling approach may be estimated by assessment of the quality of the generated samples (*i.e.*, quality of RNA- or protein isolates, preservation of the histomorphological and ultrastructural properties of tissue samples, their suitability for immunohistological analyses, *etc.*)[2]

Generation of Isotropic Uniform Random (IUR) Sections and Vertical Uniform Random (VUR) Sections for Quantitative Stereological Analyses

The techniques demonstrated for a forward-oriented generation of isotropic uniform random (IUR) sections and VUR sections from porcine (biobank) tissue samples (protocol step 3, **Figure 8**, **Figure 9**, **Figure 10**, **Figure 11**), allowing for examination of most quantitative stereological parameters, can quickly be accomplished with some practice, and without reasonable difficulties or sources of error. Therefore, the generation of IUR-samples shown in **Figure 9** (isector technique) and **Figure 10** (orientator technique) is fully representative for these method(s).

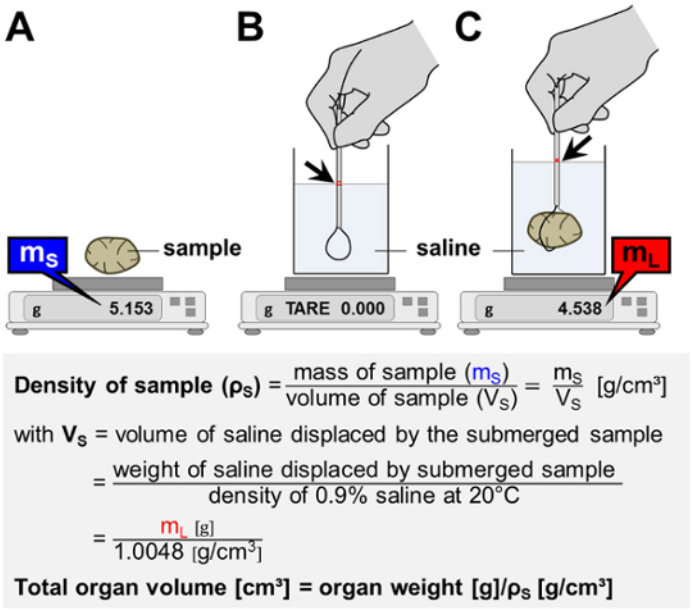

Figure 1: Schematic illustration of the "Submersion technique" for determination of tissue/organ densities. (**A**) Measurement of the sample weight (*i.e.*, mass, m_S). (**B**) Scale tared to the weight of a beaker filled with 0.9% saline of 20 °C and a sample holder submerged in the saline to a defined, marked position. (**C**) Complete submersion of the sample to the marked position of the sample holder without any contact to the inner walls or the bottom of the beaker. The weight displayed at the balance is the weight of the volume of saline displaced by the sample). The density of the sample is calculated as indicated (here: $\rho_{sample} = m_S/V_S = m_S/(m_L/1.0048) = 5.153/(4.538/1.0048) = 1.141$ g/cm³). Please click here to view a larger version of this figure.

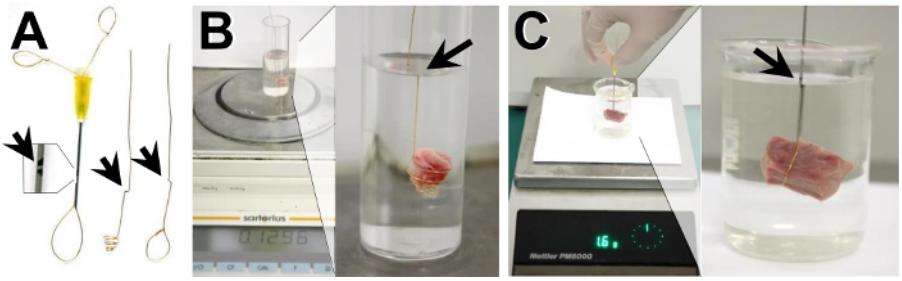

Figure 2: "Submersion technique" for determination of tissue/organ densities. (**A**) Different sample holders constructed from thin wire.From left to right:a loop of thin wire thread through a thin injection cannula, a helical basket of wire to hold small and fragile specimens, and a simple sling of thin wire. Arrows in **A**-**C** indicate the positions to which the sample holders are submerged into saline. (**B**, **C**) Positioning of the sample holder during submersion of the sample in saline (compare to **Figure 1 C**). (**B**) Complete porcine pituitary gland placed in a basket-shaped sample holder. (**C**) Sample of porcine myocardium. Note the complete submersion of the samples in saline without contacting the walls or the bottom of the beaker. Please click here to view a larger version of this figure.

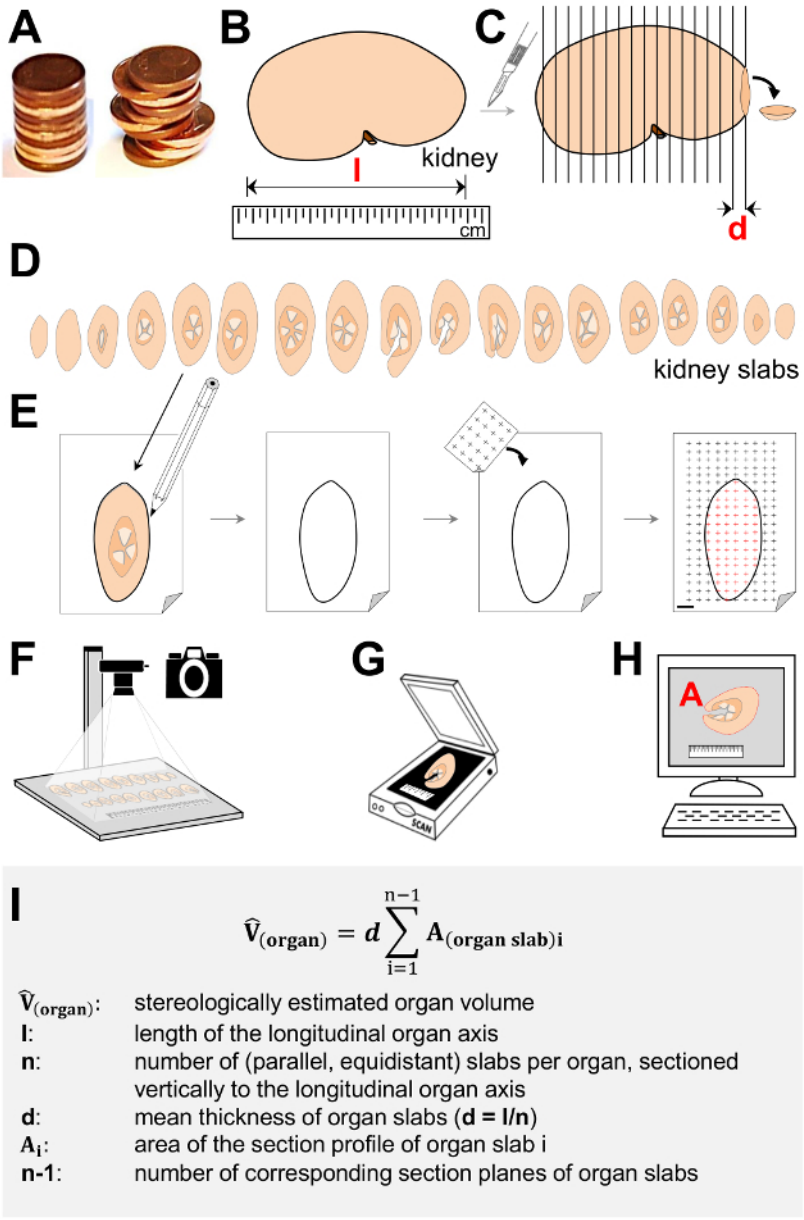

Figure 3: Schematic illustration of the application of the Cavalieri method for determination of porcine organ volumes. (**A**) Coin stack example for the comprehension of the Cavalieri principle. See Introduction for details. (**B-H**) Schematic demonstration of volume estimation of a perfusion-fixed kidney. (**B**) Measurement of the length (*l*) of the kidney along its longitudinal axis. (**C**) Cutting of the complete organ into *n* equally thick (*d*) parallel slices orthogonal to the longitudinal organ axis. (**D**) Organ slabs placed on the same surface facing down. Note that the first (right) tissue slab is placed on its natural surface, *i.e.*, does not have a section surface. (**E**-**H**) Different approaches to determine the section surface areas of the tissue slabs. (**E**) Tracing the outline of every organ slab with a waterproof pen on a plastic transparency overlay of the outlined organ slab profiles with an appropriately sized, calibrated cross grid printed on a plastic transparency, counting of crosses hitting the profile area. The organ slab section profile area is calculated from the number of crosses hitting the section profile area and the area corresponding to one cross. (**F**,**G**) Determination of section areas of the organ slabs in photo images taken in vertical orientation to the section surfaces (**F**), or in scanned images of the tissue slabs (**G**), with rulers for calibration. (**H**) Determination of the section areas of the tissue slabs in the digital images of the photos/scans using appropriate morphometry software applications. (**I**) Calculation of the estimated volume of the organ as the product of the cumulative area of the corresponding section surfaces of all organ slabs multiplied by the mean thickness of the organ slabs[15]. Please click here to view a larger version of this figure.

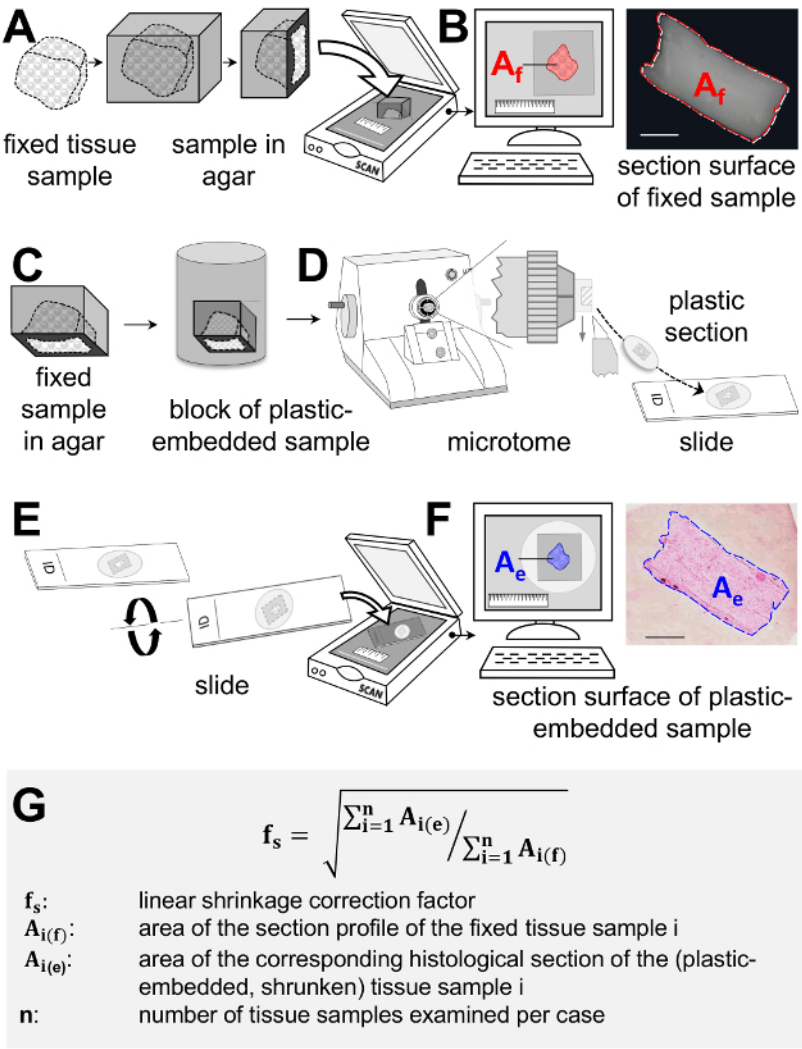

Figure 4: Schematic illustration of determination of three-dimensional embedding-related tissue shrinkage during processing of tissue samples for histology. (**A**) Cutting of a fresh, plane section surface from a fixed tissue sample (stabilization of the shape of easily deformable (soft) tissues such as adipose or lung tissue by embedding in agar prior to sectioning). Scanning of the section surface of the sample together with a size ruler. (**B**) Planimetric determination of the area of the section surface of the fixed tissue sample (A_f). (**C**) Routine embedding of the sample in plastic embedding medium. (**D**) Preparation of a histological section of the plastic block with preservation of the section plane of the sample. Mounting of the section on a glass slide and routine staining of the slide. (**E**) Scanning of the slide together with a size ruler. (**F**) Planimetric determination of the area of the section of the plastic-embedded sample (A_e). (**G**) Calculation of the extent of embedding-related tissue shrinkage as the quotient of the measured areas of corresponding section profiles of tissue samples before and after embedding in plastic embedding medium[14]. Images on the right side show the section surface of a formaldehyde-fixed sample of fat tissue embedded in ink-blackened agar before embedding in plastic resin (top) and the corresponding section profile (HE-staining) of the GMA/MMA-embedded sample (bottom). Scale bars = 2 mm. Please click here to view a larger version of this figure.

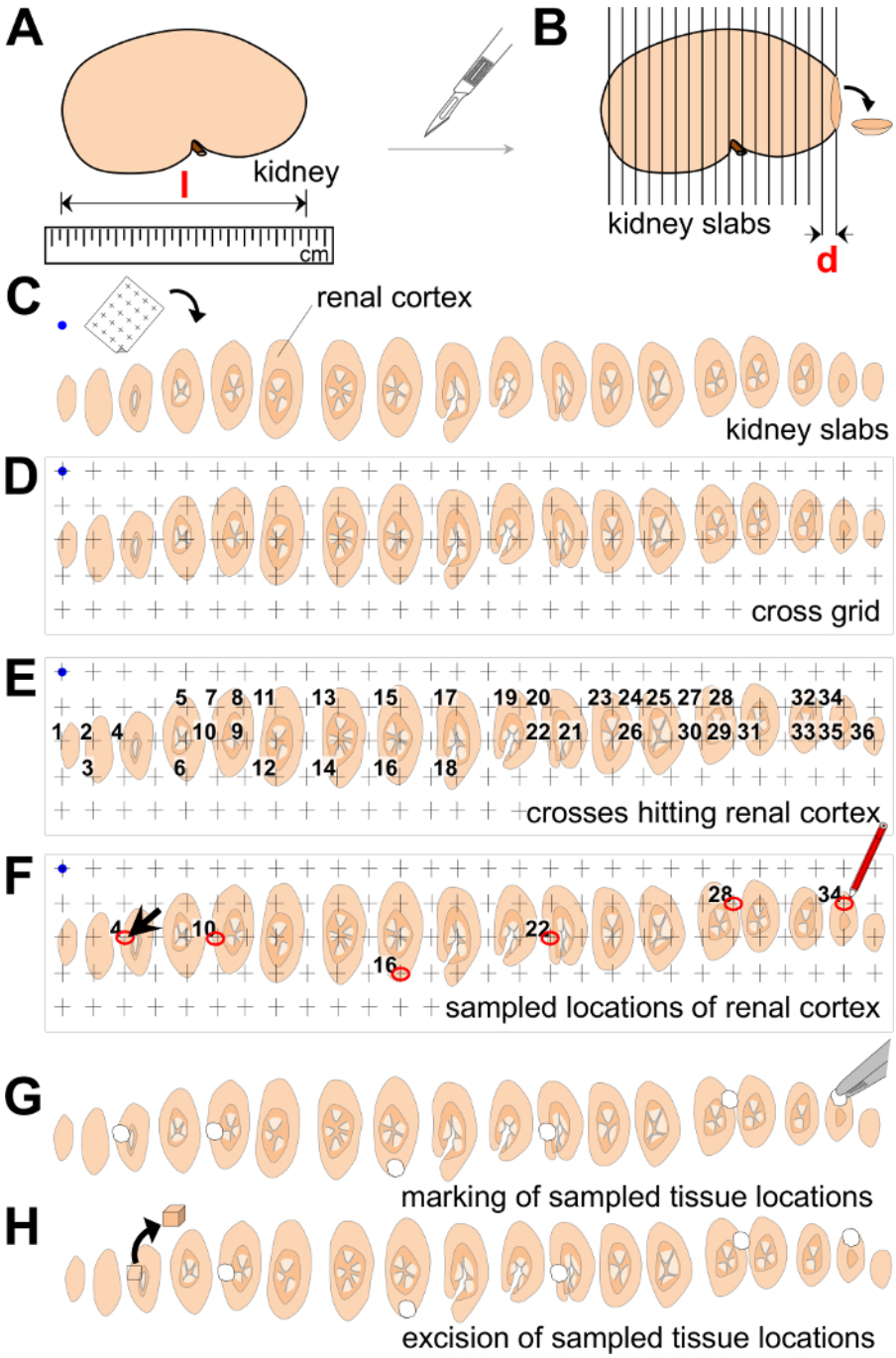

Figure 5: Schematic illustration of volume-weighted systematic random sampling. The presented example shows systematic random sampling of six tissue locations within the renal cortex of a perfusion-fixed kidney. (**A**) Measurement of the length (*l*) of the kidney along its longitudinal axis. (**B**) Complete sectioning of the entire organ into equally thick (*d*) parallel slices orthogonal to the longitudinal organ axis. (**C**) Organ/tissue slabs placed on the same (*i.e.*, either the right or the left) surface facing down. (**D**) Overlay ofthe tissue slabs with an appropriately sized cross grid printed on a plastic transparency. The outermost left upper cross of the grid is placed over a random point outside the tissue (indicated by a blue dot, •). (**E**) Counting and numbering of all crosses hitting the renal cortex. In the present example, the crosses hitting the renal cortex are numbered consecutively in one kidney slab after another (from the left to the right), in each slab proceeding in clockwise direction, starting with the cross closest to the twelve o'clock position. Here, 36 crosses hit the renal cortex. Six sampling positions are to be sampled. Therefore, every sixth position where a cross hits the tissue is sampled (36/6 = 6). (**F**) In the present example, the position of the fourth cross (N° 4) hitting the renal cortex is randomly chosen as the first sampling position. Every following sixth cross hitting the renal cortex is marked on the plastic transparency using a waterproof pen. In the present example, these are the positions 4, 10, 16, 22, 28, and 34. (**G**) Tagging of the corresponding tissue locations by small pieces of clean, blank confetti paper placed on the surface of the tissue. (**H**) Excision of tissue specimens from the randomly systematically sampled locations and subsequent processing for further analyses. This figure has been modified from Albl et al. (2016), figures S236 and S237, page 186 (supplements)[7]. Please click here to view a larger version of this figure.

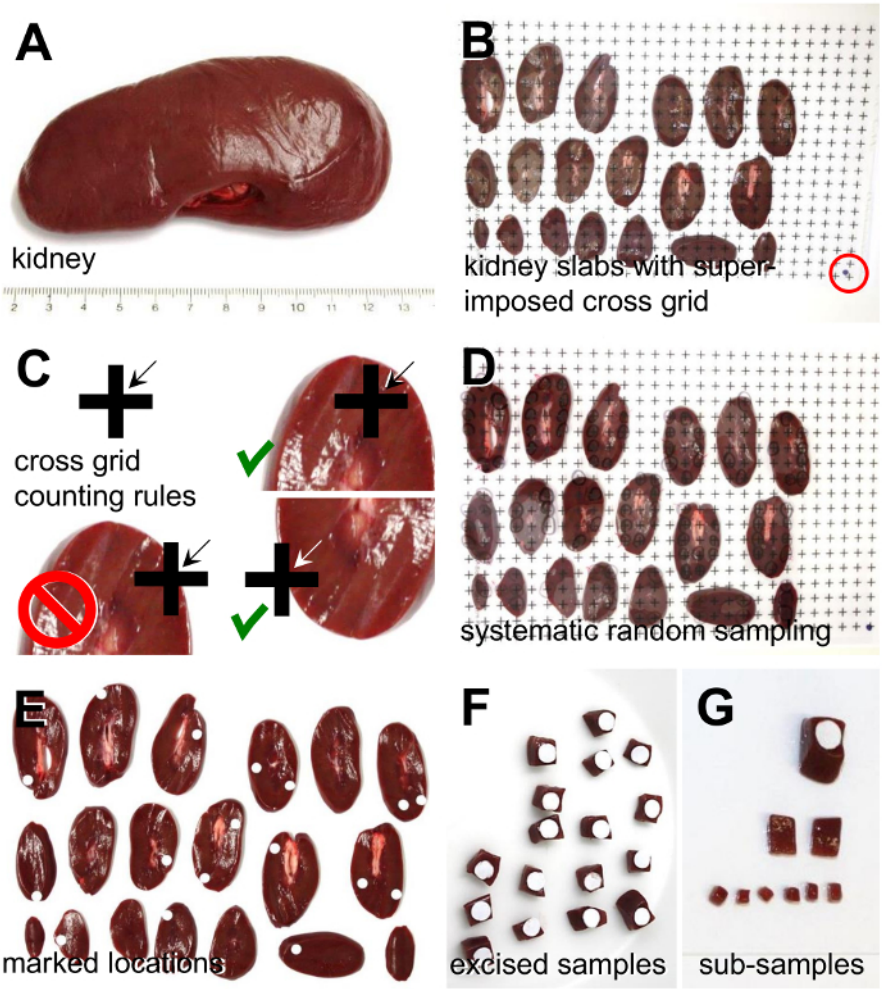

Figure 6: Volume-weighted systematic random sampling of the renal cortex of a porcine kidney (refer to Figure 5) and rules for point-counting. (**A**) Fresh pig kidney. (**B**) Kidney sectioned into equally thick parallel slices orthogonal to the longitudinal organ axis, overlaid with cross grid printed on a plastic transparency. The red circle indicates the position of the random point used to randomize the position of the cross grid. (**C**) Illustration of point-counting rules: A cross/point is counted as hitting the tissue compartment to be sampled (reference compartment), if the right upper inner corner of the vertical and horizontal bar of the cross (arrow) covers the tissue. (**D**) Marking of crosses hitting the renal cortex and systematic random sampling of tissue locations (here, 119 crosses hit the renal cortex and 17 locations are systematically randomly sampled using a sampling interval *i* = 7). (**E**) Randomly systematically sampled locations of renal cortex tagged by confetti paper. (**F**) Excised samples. (**G**) Further subdivision of excised samples for subsequent processing of subsamples for different downstream analysis types. Please click here to view a larger version of this figure.

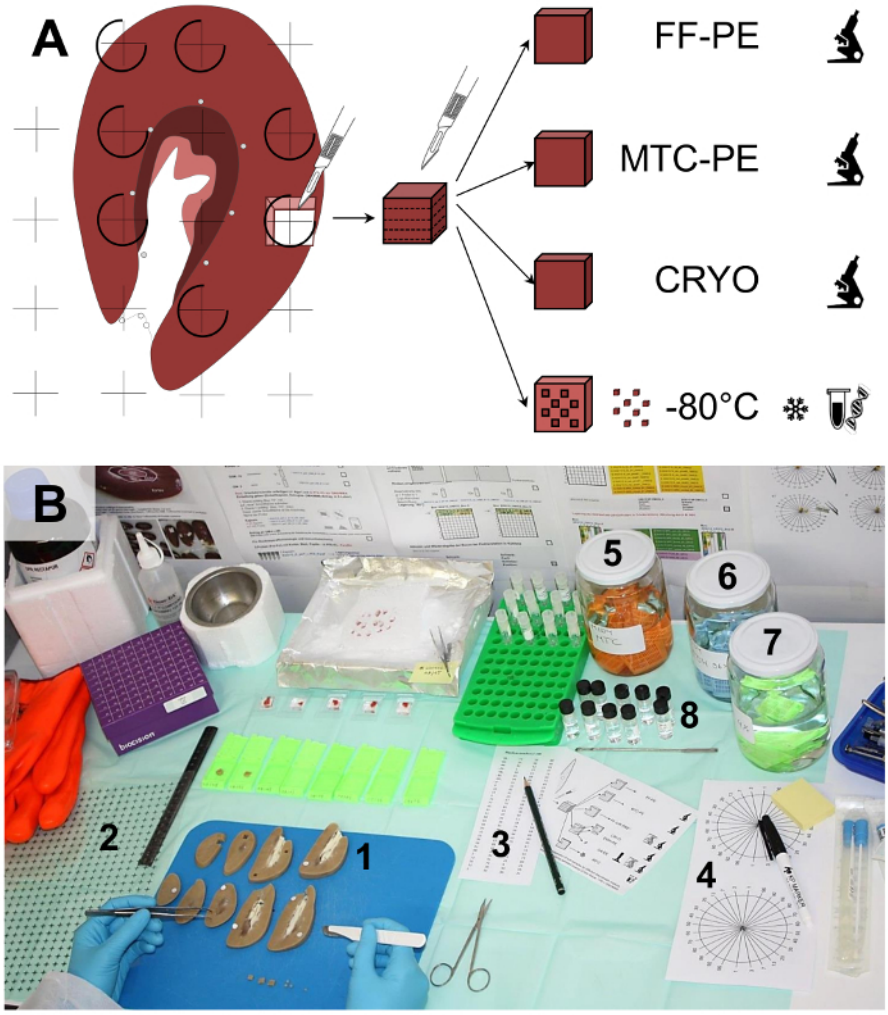

Figure 7: Subdivision of tissue samples excised from systematically randomly sampled tissue locations and processing of subsamples for different downstream analysis types. (**A**) Schematic illustration of generation of tissue subsamples from one systematically randomly sampled location of renal cortex (native tissue) for different analyses (*e.g.*, FF-PE: Formalin-fixed, paraffin-embedded sample, and MTC-PE: Methacarn-fixed, paraffin-embedded sample for light-microscopic histology; CRYO: Sample for frozen section histology; -80 °C: Dry-ice frozen tissue samples for molecular analysis). (**B**) Excision of systematically randomly sampled locations of the renal cortex of a perfusion-fixed kidney, further subdivision of the excised tissue samples, and processing of the subsamples for qualitative and quantitative morphological analyses. Slabs of perfusion-fixed porcine kidney (1), cross-grid (2), random number table (3), equiangular and cosine-weighed circles (4) for generation of IUR sections (see **Figure 9**, **Figure 10**), different fixation solutions (5, 6, 7), and sample container for electron microscopic samples (8). This figure has been modified from Albl *et al.* (2016), figure S239, page 186 (supplements)[7]. Please click here to view a larger version of this figure.

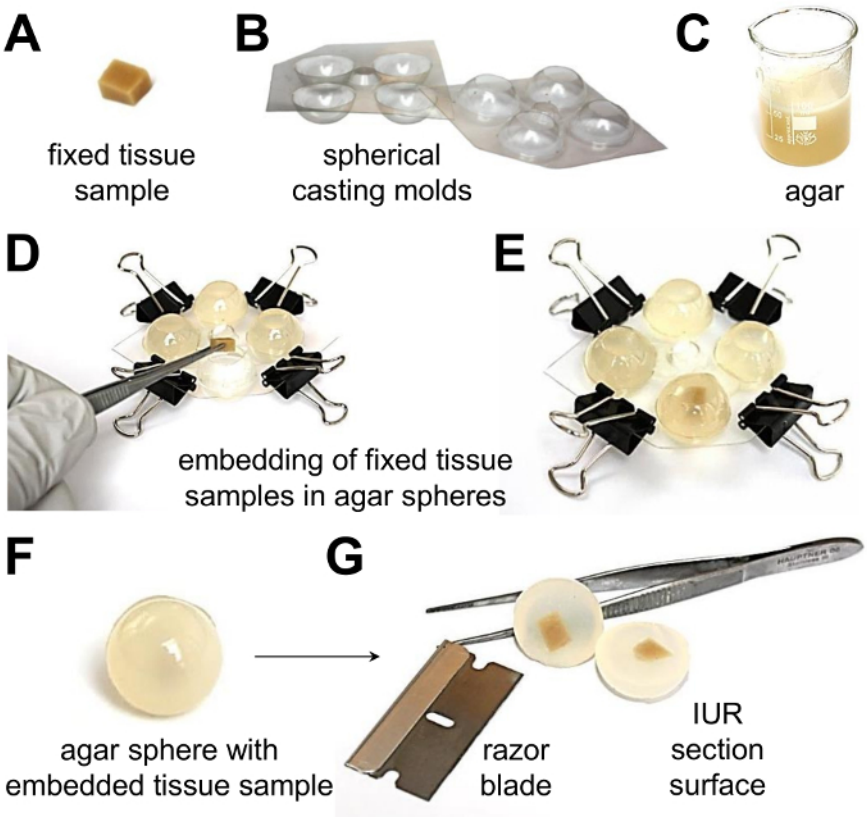

Figure 8: "Isector" section preparation from formalin-fixed porcine tissue. (**A**) Sample of perfusion-fixed porcine renal cortex. (**B**) Spherical casting molds. (**C**) Liquid agar. (**D-E**) Agar-embedding of samples in spherical casting molds. (**F**) Agar sphere with embedded tissue sample. (**G**) Agar sphere with embedded tissue sectioned at a random position (IUR section plane). This figure has been modified from Albl *et al.* (2016), figure S6, page 14 (supplements)[7]. Please click here to view a larger version of this figure.

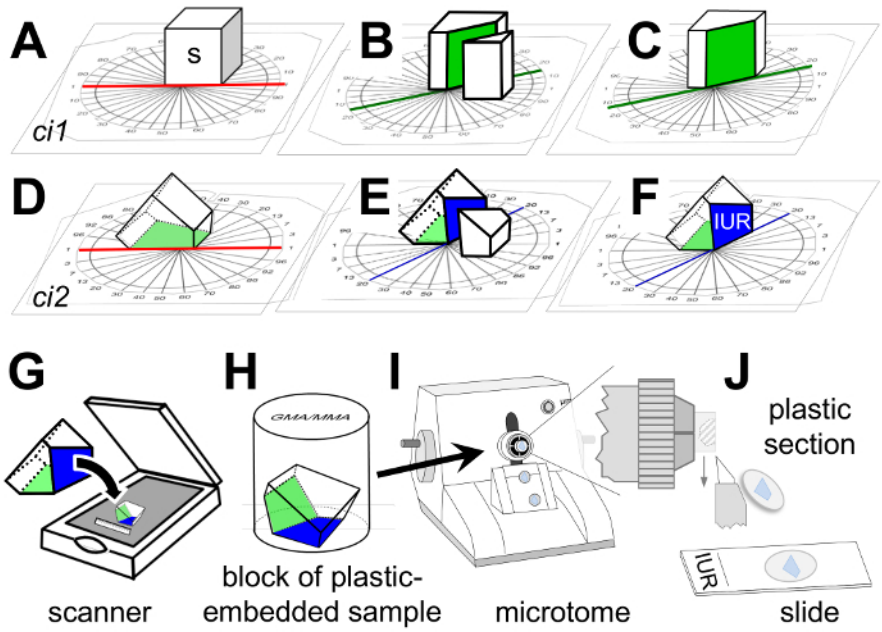

Figure 9: Schematic illustration of the "Orientator" technique for preparation of IUR sections. (**A**) Sample(s) of fixed tissue placed on an equiangular circle (*ci1*) with an edge parallel to the 0–180° direction (indicated by a red line). (**B**) Sectioning of the sample at a random angle (green line). (**B,C**) Newly generated section surface of the tissue sample (indicated in green color). (**D**) Sample placed on a cosine-weighed circle (*ci2*) with the sectional surface generated in the previous step facing downside and one edge of the resting surface parallel to the 1-1 direction (indicated by a red line). (**E**) Cutting of the second section through the sample at a random angle. (**F**) Resulting randomly isotropic section plane of the sample (indicated in blue color). (**G**) Determination of the area of the IUR section of the fixed tissue sample for estimation of embedding-related tissue shrinkage as described in step 1.3. (**H**) Embedding of the tissue sample in plastic resin. (**I**) Sectioning of the plastic block is sectioned (parallel to the IUR plane) on a microtome. (**J**) Mounting of the IUR plastic-sections on glass slides. This figure has been modified from Albl *et al.* (2016), figure S8, page 15 (supplements)[7]. Please click here to view a larger version of this figure.

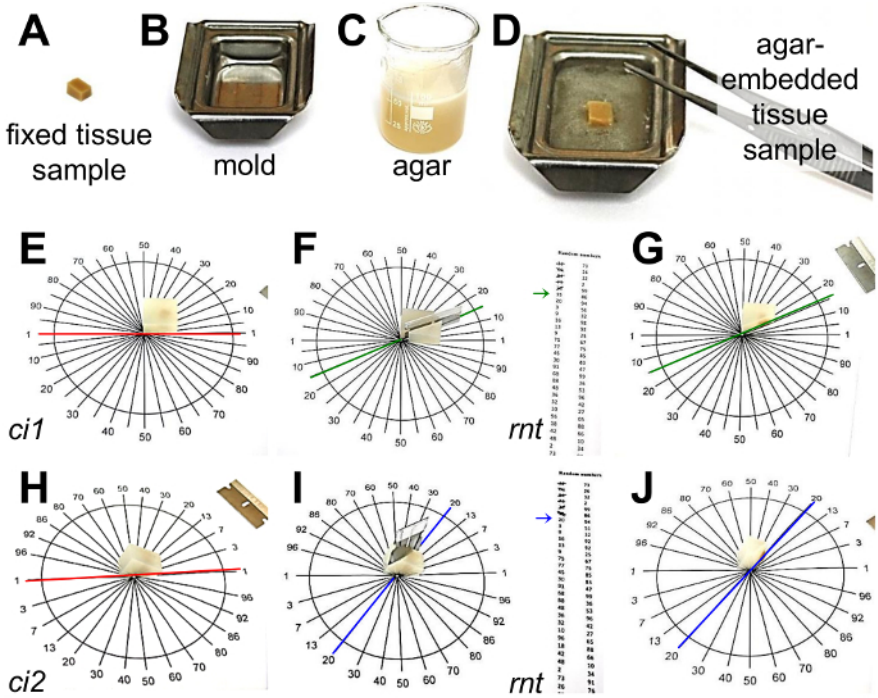

Figure 10: "Orientator" technique for preparation of IUR sections of agar-embedded tissue samples. (**A-D**) Optionally, one may agar-embed a systematically randomly sampled specimen of fixed tissue (agar-embedding is useful for small tissue samples, so that the first or both random sections can be positioned within the agar without cutting the tissue). (**E**) Positioning of the agar block on an equiangular circle (*ci1*) with an edge parallel to the 1-1 direction (indicated by a red line). (**F, G**) Sectioning of the block at a random angle (here: 15-15, green line) determined using a random number table (rnt, green arrow). (**H**) Subsequent positioning of the agar block on the section surface cut in **F** on a cosine-weighted circle (*ci2*) with the edge of the resting surface placed parallel to the 1-1 direction (indicated by a red line). (**I**) Second section cut through the sample at a random angle (here: 20-20, indicated by a blue line), determined by using a random number table (rnt, blue arrow). (**J**) Resulting IUR section plane of the tissue sample. This figure has been modified from Albl *et al.* (2016), figure S9, page 16 (supplements)[7]. Please click here to view a larger version of this figure.

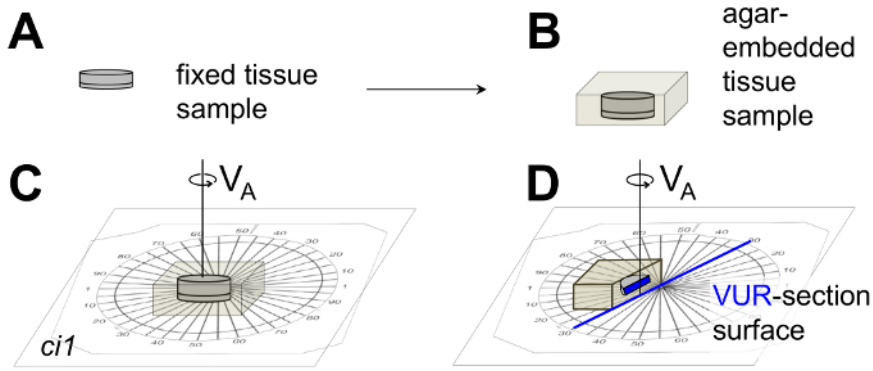

Figure 11: Schematic illustration of VUR section preparation. (**A**) Fixed tissue sample with a defined (identifiable) vertical axis (*e.g.*, vertical to its natural surface). (**B**) Fixed tissue sample embedded in agar. (**C**) Positioning of the(agar-embedded) tissue sample on a print of an equiangular circle (*ci1*). V_A: Vertical axis. (**D**) Sectioning of the sample at a random angle (random number table; here: 30-30 direction, indicated by a blue line) with the section plane being orthogonally oriented to the table and parallel to the vertical axis of the sample. Resulting VUR section plane of the tissue sample (indicated in blue color). Please click here to view a larger version of this figure.

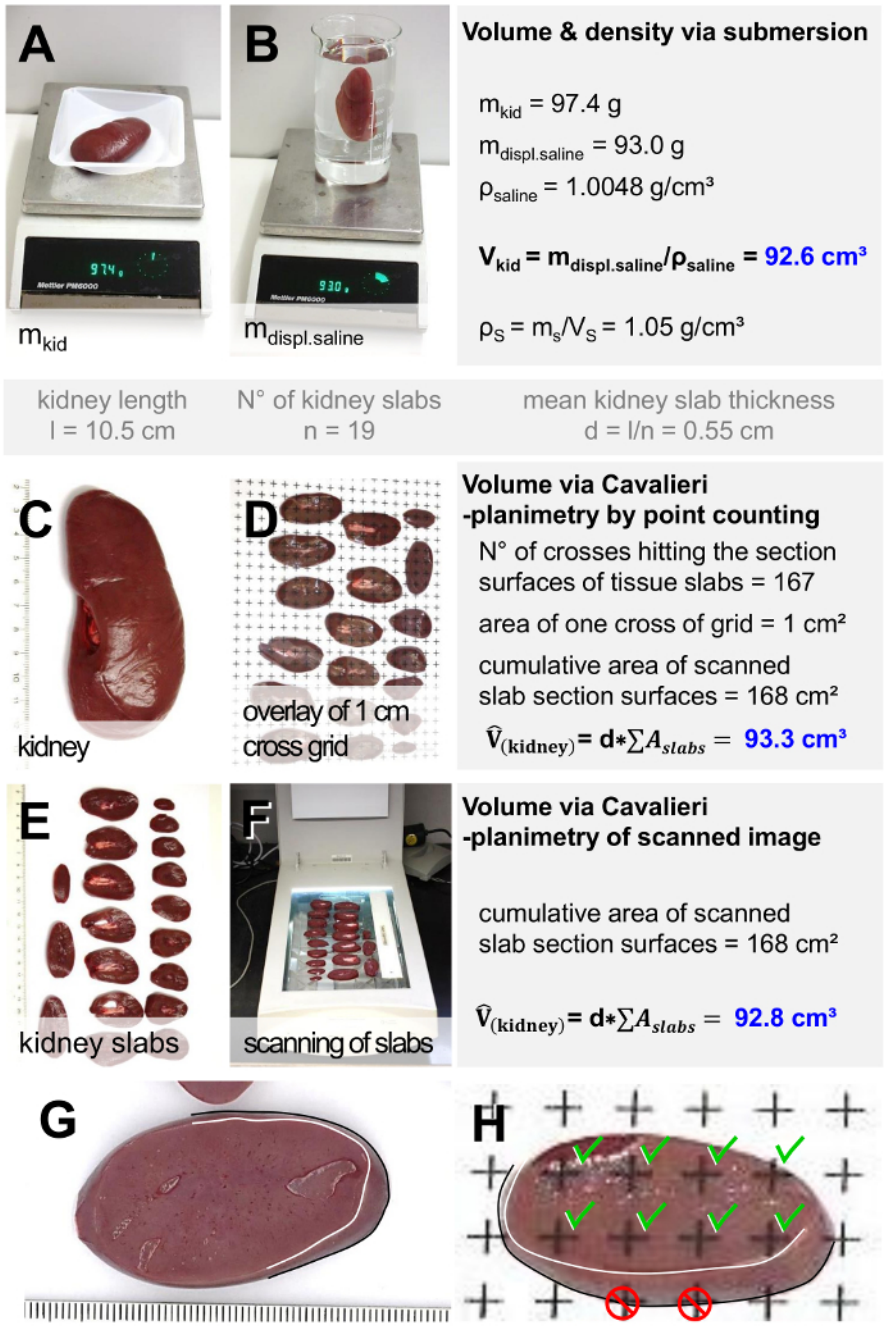

Figure 12: Representative volumetry of a porcine kidney. (**A**-**B**) Submersion technique. (**A**) Determination of the kidney weight (m_{kid}). (**B**) Determination of the weight of the volume of saline displaced by the kidney ($m_{displ.saline}$). The kidney is hung on a string and fully submerged in saline without touching the bottom or the walls of the beaker. The calculated volume of the kidney is 92.6 cm³. (**C**-**D**) Cavalieri technique, planimetry by point-counting. (**C**) Measurement of the length (l) of the kidney along its longitudinal axis. (**D**) Determination of the section profile areas of the kidney slabs by point counting after overlay of a grid of equally spaced crosses printed on a plastic transparency. Here, the estimated volume of the kidney is 93.3 cm³. (**E**-**F**) Cavalieri technique, planimetry of scanned images of section profile areas of the kidney slabs (**F**). Here, the estimated volume of the kidney is 92.8 cm³. In **C**-**E**, the natural round surface of the first or the last slab of the kidney placed on the scanner or overlaid by the cross grid transparency is not a section surface and therefore, no section surface area is measured in this tissue slab. (**G**-**H**) Demonstration of overprojection in scanned images of organ/tissue slabs (**G**) and in organ/tissue slabs overlaid with a cross grid transparency (**H**). Overprojecting parts of the tissue of the organ slabs are indicated by dotted white and black lines. Only the areas of the actual section profiles (*i.e.*, the tissue surrounded by the partially indicated white dotted line) are determined. Please click here to view a larger version of this figure.

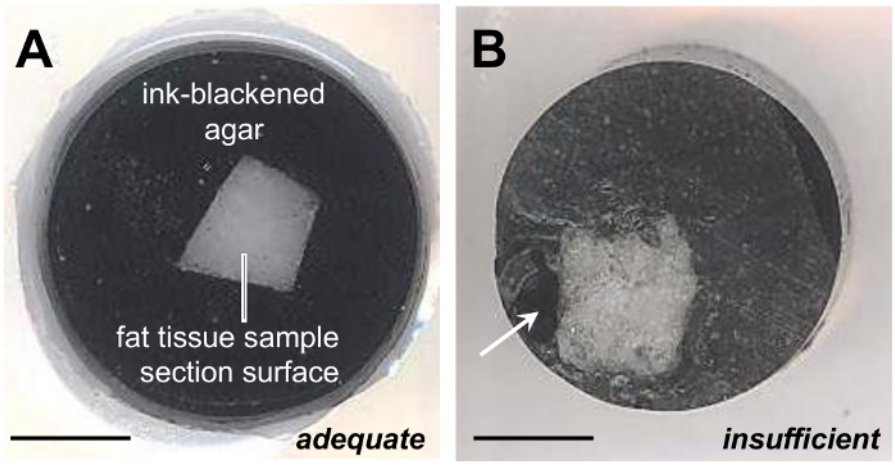

Figure 13: Representative illustration of adequate (A) and suboptimal (B) preparation of agar-embedded tissue samples for determination of tissue shrinkage related to embedding of samples in histological plastic embedding media. (**A**) Scanned image of the section surface of a fixed sample of porcine subcutaneous adipose tissue prior to embedding in plastic resin. The sample is embedded in ink-blackened agar for stabilization of the shape of the sample and clear identification of the section surface contours. (**B**) Indistinct outline of the section surface and entrapped air bubble (arrow) within the agar. Scale bars = 5 mm. Please click here to view a larger version of this figure.

Analysis		**Sample**	**Processing**
Type	**Method(s)**		
Molecular analyses	**RNA transcript, protein, metabolite, and lipid profiling, metabolomics analysis, DNA analysis**	Small pieces* of fresh (native) tissue	Freeze on dry ice or in liquid nitrogen. Store at -80 °C.
Qualitative morphological analyses	**Histology** [light microscopy, incl. immunohistochemistry (IHC) & in situ hybridization]	Fresh (native) — or *in situ* - fixed* tissue samples	Use different fixatives (*e.g.*, 4% formaldehyde solution) and embedding media (paraffin, GMA/MMA, epoxy), as appropriate.
	Cryohistology (frozen sections, incl. IHC)	Fresh (native) tissue samples	Embed sample in blocking medium and freeze in liquid nitrogen-cooled isopentane.
	Ultrastructural analysis [electron microscopy, incl. transmission- (TEM) and scanning electron microscopy]	Small pieces of fresh (native) — or *in situ*- fixed* tissue samples	Fix sample in 2.5–6.25% glutaraldehyde solution and embed in epoxy plastic resin.
Quantitative morphological analyses	**Light microscopy**	Fresh (native) - or *in situ* - fixed* tissue samples	Prepare IUR-sections (orientator-, isector-sections) and/or VUR-sections of plastic embedded tissue samples.
	TEM	Small pieces of fresh (native) — or of *in situ* - fixed* tissue	Prepare IUR (orientator-, isector-sections) sections of epoxy-embedded tissue samples.

Table 1: Processing of tissue subsamples excised from systematically randomly sampled locations for different downstream analyses types. Depending on the experimental design of a study and the organ/tissue under investigation, different numbers of subsamples should be excised from each systematically randomly sampled tissue location and processed for different types of downstream analyses. Detailed protocols for most porcine organs/tissues and study types are provided in the "Tissue Sampling Guides for Porcine Biomedical Models"[7]. GMA/MMA: Glycolmethacrylate/methylmethacrylate. IUR: Isotropic uniform random. VUR: Vertical uniform random. * max. 2 x 2 x 2 mm^3. ** *e.g.*, perfusion fixed tissue or pulmonary tissue of lungs instilled with fixation solution.

Method	Representative results		
Submersion technique for determination of tissue/organ densities (step 1.1, **Figure 1**, **Figure 2**)	**Porcine organ/tissue**		**ρ (g/cm³)**
	Liver		1.071 ± 0.007
	Pancreas		1.062 ± 0.016
	Ventricle myocardium		1.036 ± 0.014
	Kidney		1.044 ± 0.006
	Abdominal visceral adipose tissue*		0.921 ± 0.032
	Thyroid gland		1.061 ± 0.007
	Brain		1.051 ± 0.007
	Adrenal gland		1.063 ± 0.025
	Skeletal muscle**		1.074 ± 0.003
	Data are means ± SD. Specific organ/tissue weights were determined in n = 18 pigs (14 female and 4 male pigs; age 60 days to 2 years; body weight 30–250 kg). *Adipose tissue from the jejunal mesentery. **Mean values for the M. longissimus dorsi, M. tibialis cranialis, M. triceps brachii, and M. gluteobiceps.		
Determination of three-dimensional embedding-related tissue shrinkage during processing of tissue samples for histology (step 1.3, **Figure 4**)	**Organ/tissue**	**Embedding medium**	**f_S**
	Renal cortex (pig)	GMA/MMA	0.89 ± 0.02
		Epoxy	0.92 ± 0.02
	Data are means ± SD of measurements of 24 samples of 12 pigs. f_S: Linear shrinkage correction factor.		

Table 2: Representative results of densities of selected porcine organs and tissues[7], and linear shrinkage correction factors for embedding-related tissue shrinkage of porcine cortical kidney tissue in different plastic embedding media.

Discussion

Generation of biobank sample collections from porcine animal models requires robust techniques and protocols for the determination of organ/tissue volumes, the reproducible generation of representative, redundant tissue samples suitable for a broad range of different analysis methods, and for randomization of the orientation of sample sections for quantitative stereological analyses. The methods described in the present article are adapted to the sizes of porcine organs and tissues, and have been developed to effectively meet these demands[2,7]. They are based on well recognized methodological principles, and have previously proven their practicability in different published studies[2,7,12,21]. The featured methods are important for various types of studies examining tissue/organ samples, since they provide a basis for generation of representative samples, and for acquisition of a variety of parameters which could otherwise not be determined. These methods can quickly be performed with little effort, and are compatible with virtually all kinds of downstream analyses. Therefore, they are considered suitable not only for porcine animal model biobank projects, but also are useful in studies involving quantitative histomorphological analyses of tissue samples of other large animal model species (*e.g.*, sheep), as well as in veterinary studies. Taking the technical aspects of the different methods into account, a few critical steps and limitations have to be considered during implementation of the protocols of the respective techniques.

Submersion technique for determination of tissue/organ density

During determination of tissue densities using the submersion method (step 1.1, **Figure 1**, **Figure 2**), care must be taken not to touch the inner walls or the bottom of the beaker with the tissue sample or the sample holder while the tissue sample is submerged in saline. Otherwise, the scale will display the weight of the sample rather than the weight of the volume of saline displaced by the sample. For very small/light tissue samples (a few mg), the submersion method for determination of tissue density is limited, due to the surface tension of the saline and the adversely high quotient of sample volume to the volume of submersion liquid in the beaker, which is impeding the accuracy of the measurement. Here, the weight of the sample might be used for further calculations instead of the density-calculated volume. Determination of tissue densities by submersion is also not effective for fresh (unfixed) lung tissue, due to the inconsistent content of air in the tissue, and in some cases, where organs are experimentally perfused/instilled with fixatives.

Cavalieri method for determination of organ volumes

The method of Cavalieri volumetry of porcine organs and tissues is more cumbersome when compared to determination of the organ volume from the organ weight and density. However, it is suitable for organs that cannot appropriately be weighed due to their experimental processing (*e.g.*, perfusion-fixed organs, or lungs instilled with fixation solution). Here, the Cavalieri volumetry method can ideally be combined with the volume-weighted systematic random sampling technique described in step 2 (**Figure 5**, **Figure 6**, **Figure 12**). During estimation of organ/tissue volumes from the areas of section profiles of parallel, equidistant slices of the organ/tissue (Cavalieri approach, step 1.2, **Figure 3**), maintenance of the orientation of the tissue slabs (upper and lower section plane), as well as the accurate determination of the area of all section profiles are of great importance. Particularly, if digital images or scans of organ slabs are analyzed planimetrically, overprojections of tissue (outside of the sectioned tissue plane) of the tissue slab (**Figure 12G-H**) must carefully be considered to provide reliable volume estimates.

Determination of three-dimensional embedding-related tissue shrinkage during processing of tissue samples for histology

The extent of embedding-related tissue shrinkage depends on the embedding medium and the type of tissues, and may also vary between differentially processed samples of the same tissue.

Whereas frozen sections are considered to display virtually no shrinkage in the X-Y plane, and plastic embedding generally causes little shrinkage of the tissue, embedding-related tissue shrinkage is particularly extensive in paraffin-embedded tissue samples, and will usually significantly impair quantitative morphological analyses of dimensional parameters in histological sections of these samples. In addition to the large extent of overall three-dimensional shrinkage, paraffin-embedding also causes a non-uniform, differential, anisotropic, and variable shrinkage of the sample and of different anatomical structures, tissue types and cell types within the tissue sample[8,13]. Moreover, particularly in thicker histological sections of paraffin-embedded tissue samples, the extent of tissue shrinkage may also significantly differ in the X-Y and the Z-direction of the section. This can be due to a differential shrinkage of the section area (in X-Y-direction) and the section height (*i.e.*, the vertical section thickness) during stretching of the section in the warm tissue flotation water bath after the section is cut from the tissue block, and during the subsequent processing, staining, and coverslipping procedures of the section mounted on a glass slide (*i.e.*, a homogenous collapse of the sections' Z-axis)[8]. Additionally, in thick sections, there might be a comparably stronger compression of the section-plane-near tissue regions within the section while the section is cut from the tissue block (leading to a differential deformation of the sections' Z-axis)[19]. These effects may then also distort the estimates of the number of tissue structures within the section by distinct quantitative stereological analysis methods, such as the optical disector. Therefore, prediction, monitoring, and correction of embedding-related tissue shrinkage is not feasible for paraffin-embedded tissue samples[8].

In contrast, the extent of volume shrinkage of tissue samples embedded in plastic resins, such as GMA/MMA or epoxy, is significantly lower and, importantly, more uniform. Therefore, embedding in plastic resin with an assumed homogenous, isotropic, and global shrinkage of the tissue is advantageous for several analysis methods of different quantitative morphological parameters[17,18]. During estimation of tissue shrinkage related to embedding in plastic resin, the shape of the fixed tissue should not additionally be distorted during the embedding procedure, to allow for comparison of corresponding section profile areas of the fixed and embedded samples. This can be difficult in soft or easily compressible tissue samples such as adipose or lung tissue, or in tissue samples with a high fluid content. Here, embedding of the fixed sample in agar prior to sectioning of the tissue is helpful to stabilize the shape of the tissue sample during the subsequent plastic embedding procedure (protocol step 1.3., **Figure 4**). To achieve reliable data, repeated measurements of the embedding-related tissue shrinkage should be performed, using different samples of the same tissue. The extent of embedding-related tissue shrinkage is expressed as the linear tissue shrinkage factor f_s (protocol step 1.3.9., **Figure 4G**). Examples for equations using f_s for shrinkage correction of various length, surface area, and volume parameters of different tissue structures are provided in several quantitative stereological studies[14,21,27].

Volume-weighted systematic random sampling by point counting and processing of tissue subsamples for different downstream analysis types

The presented volume-weighted sampling technique for porcine organs determines random sampling locations within the tissue once, and subsequently generates all necessary samples for further different analyses by subsampling of the tissue samples excised from these locations[7]. In volume-weighted systematic random sampling regimes, each possible sampling location within the total volume of the organ/tissue under examination has exactly the same random chance to be sampled, and generalizability is ensured by the collection of a sufficient number of specimens. Using volume-weighted systematic random sampling designs for generation of samples from parenchymal organs, therefore, effectively prevents analysis results possibly biased by (potentially unexpected and unrecognized) unequal distributions of distinct functional or morphological tissue properties within different locations of an organ, which have been demonstrated, *e.g.*, for the mean volume and the numerical volume density of porcine hepatocytes in different regions of the liver parenchyma[28]. The featured "tissue-slabbing and subsampling" strategy for porcine organs is easily comprehensible, complies with the technical requirements of the downstream analyses methods, and can be quickly carried out and adapted to the demands of a specific study, thereby avoiding systematic sampling biases, reducing experimental variability, and increasing the precision of the overall experiment, while being more efficient than sampling strategies in which each single sampling location is determined randomly[9,15]. The number of specimens that have to be generated, obviously depend on the examined parameter and its variability within samples from different locations of the sampled organ/tissue. For generation of biobank sample collections designed to allow for examination of a maximum of different parameters (not specified at the time of sampling) by a variety of different analytical methods, such a forward-looking sampling strategy usually schedules generation of relatively high numbers of redundant samples per organ/tissue.

Generation of Isotropic Uniform Random (IUR) sections and Vertical Uniform Random (VUR) sections for quantitative stereological analyses

Some of the techniques used for generation of IUR and VUR sections for quantitative stereological analyses have somewhat complicated theoretical bases, and explanations are therefore often (unnecessarily) eschewed by many scientists, although their practical implementation is reasonably easy. VUR sections are particularly easy to generate, and are optimal for surface density/area estimations in combination with cycloid test systems[8,9,20]. They are often preferred due to the familiar orientation of the section plane. However, in contrast to IUR sections, VUR sections are not suitable for estimation of length-parameters[8,9].

During preparation of IUR and VUR sections, the critical step is, basically, to maintain the IUR or VUR section surface of the fixed sample during embedding in plastic resin, and to ensure that the vertical axis of VUR sections can always be identified (step 3, **Figure 9, Figure 10, Figure 11**).

In the future, the broader application of the methods described above might substantially contribute to establish consistently high-quality standards for generation of comparable, multi-purpose biobank samples from porcine and other large animal models.

Disclosures

The authors have nothing to disclose.

Acknowledgements

The authors thank Lisa Pichl for excellent technical assistance.

References

1. Aigner, B. et al. Transgenic pigs as models for translational biomedical research. *J Mol. Med.* **88**, 653-664 (2010).
2. Blutke, A. et al. The Munich MIDY Pig Biobank: A unique resource for studying organ crosstalk in diabetes. *Mol Metab.* **6**, 931-940 (2017).
3. Klymiuk, N. et al. Dystrophin-deficient pigs provide new insights into the hierarchy of physiological derangements of dystrophic muscle. *Hum Mol Genet.* **22**, 4368-4382 (2013).
4. Klymiuk, N., Seeliger, F., Bohlooly, Y.M., Blutke, A., Rudmann, D.G., Wolf, E. Tailored pig models for preclinical efficacy and safety testing of targeted therapies. *Toxicol Pathol.* **44**, 346-357 (2016).
5. Renner, S. et al. Permanent neonatal diabetes in INS^{C94Y} transgenic pigs. *Diabetes.* **62**, 1505-1511 (2013).
6. Abbott, A. Inside the first pig biobank. *Nature.* **519**, 397-398 (2015).
7. Albl, B. et al. Tissue sampling guides for porcine biomedical models. *Toxicol Pathol.* **44**, 414-420 (2016).
8. Gundersen, H.J.G., Mirabile, R., Brown, D., Boyce, R.W. Stereological principles and sampling procedures for toxicologic pathologists. In: *Haschek and Rousseaux´s Handbook of Toxicologic Pathology.* 3rd ed., Haschek, W., ed., Academic Press, London, 215-286, ISBN: 9780124157590 (2013).
9. Howard, C.V. and Reed, M.G. *Unbiased Stereology: Three-Dimensional Measurement in Microscopy.* 2nd ed., Garland science/Bios Scientific Publishers, Oxford, 1-277, ISBN: 9780203006399 (2005).
10. Mattfeldt, T., Mall, G., Gharehbaghi, H., Moller, P. Estimation of surface area and length with the orientator. *J Microsc.* **159**, 301-317 (1990).
11. Nyengaard, J.R., Gundersen, H.J.G. The isector: A simple and direct method for generating isotropic, uniform random sections from small specimens. *J Microsc.* **165**, 427-431 (1992).
12. Tschanz, S., Schneider, J.P., Knudsen, L. Design-based stereology: Planning, volumetry and sampling are crucial steps for a successful study. *Ann Anat.* **196**, 3-11 (2014).
13. Dorph-Petersen, K.A., Nyengaard, J.R., Gundersen, H.J. Tissue shrinkage and unbiased stereological estimation of particle number and size. *J Microsc.* **204**, 232-246 (2001).
14. Mattfeldt, T. Stereologische Methoden in der Pathologie [Stereologic methods in pathology]. In: *Normale und pathologische Anatomie [Normal and Pathological Anatomy].* Vol. 52, Doerr, W., Leonhardt, H., eds., Georg Thieme Verlag, Stuttgart-New York, 1-3001-75, ISBN: 9783131252012 (1990).
15. Gundersen, H.J., Jensen, E.B. The efficiency of systematic sampling in stereology and its prediction. *J Microsc.* **147**, 229-263 (1987).
16. Scherle, W. A simple method for volumetry of organs in quantitative stereology. *Mikroskopie.* **26**, 57-60, PMID: 5530651 (1970).
17. Nielsen, K.K., Andersen, C.B., Kromann-Andersen, B. A comparison between the effects of paraffin and plastic embedding of the normal and obstructed minipig detrusor muscle using the optical disector. *J Urol.* **154**, 2170-2173, (1995).
18. Schneider, J.P., Ochs, M. Alterations of mouse lung tissue dimensions during processing for morphometry: a comparison of methods. *Am J Physiol Lung Cell Mol Physiol.* **306**, L341-350 (2014).
19. von Bartheld, C.S. Distribution of particles in the z-axis of tissue sections: Relevance for counting methods. *NeuroQuantology.* **10**, 66-75 (2012).
20. Baddeley, A.J., Gundersen, H.J., Cruz-Orive, L.M. Estimation of surface area from vertical sections. *J microsc.* **142**, 259-276, (1986).
21. Blutke, A., Schneider, M.R., Wolf, E., Wanke, R. Growth hormone (GH)-transgenic insulin-like growth factor 1 (IGF1)-deficient mice allow dissociation of excess GH and IGF1 effects on glomerular and tubular growth. *Physiol Rep.* **4**, e12709 (2016).
22. Rasband, W.S. *ImageJ.* U.S. National Institutes of Health, Bethesda, Maryland, USA, http://rsb.info.nih.gov/ij/, (1997).
23. Hermanns, W., Liebig, K., Schulz, L.C. Postembedding immunohistochemical demonstration of antigen in experimental polyarthritis using plastic embedded whole joints. *Histochemistry.* **73**, 439-446 (1981).
24. Romeis, B. *Mikroskopische Technik.* 17. Auflage. Böck, P., Hrsg., Urban und Schwarzenberg, München, Wien, Baltimore, 1- 697, ISBN: 3-541-11227-1 (1989).
25. Suvarna, K.S., Layton, C., Bancroft, J.D. *Bancroft's theory and practice of histological techniques.* 13th ed., Suvarna, K.S., Layton, C., Bancroft, J.D., eds., Churchill Livingstone, 1-654, ISBN: 9780702042263 (2013).
26. Knust, J., Ochs, M., Gundersen, H.J., Nyengaard, J.R. Stereological estimates of alveolar number and size and capillary length and surface area in mice lungs. *Anat Rec (Hoboken).* **292**, 113-122 (2009).
27. Nyengaard, J.R., Gundersen, H.J.G. Sampling for stereology in lungs. *Eur Respir Rev.* **15**, 107-114 (2006).
28. Junatas, K.L. et al. Stereological analysis of size and density of hepatocytes in the porcine liver. *J Anat.* **230**, 575-588 (2017).

